Journal of Applied Fluid Mechanics, Vol. 12, No. 2, pp. 631-645, 2019.
Available online at www.jafmonline.net, ISSN 1735-3645, EISSN 1735-3645.
DOI: 10.29252/jafm.12.02.28325

Computational Simulation of Shock-Bubble Interaction, using a Front-Tracking/Ghost Fluid Method

A. Razmi[1], M. Taeibi-Rahni[1,2†], H. R. Massah[3], H. Terashima[4] and H. Moezzi [1]

[1] *Department of Aerospace Engineering, Sharif University, Tehran, P.O.B. 113658539, Iran*
[2] *Aerospace Research Institute, Tehran, Iran*
[3] *Acoustical Engineering Society of Iran, Tehran, Iran*
[4] *Faculty of Engineering, Hokkaido University, Japan*

†*Corresponding Author Email: taeibi@sharif.edu*

(Received August 20, 2017; accepted October 12, 2018)

ABSTRACT

A front tracking/ghost fluid method was used to simulate fluid interfaces in a shock–bubble interaction problem. The method captures fluid interfaces, using explicit front-tracking and defines interface conditions, using the ghost-fluid method. In order to demonstrate the accuracy and the capability tracking of the approach used, an air-helium and anair-R22 shock-bubble interaction cases were simulated. The computational results were compared with reliable experimental and computational studies, showing close agreements.

Keywords: Computational simulation; Front tracking/ghost fluid method; Shock-bubble interaction; Supersonic flow.

NOMENCLATURE

D	deformation tensor
g	gravity acceleration
h	eulerian mesh size
i	indicator function
n	unit normal to the interface
u	velocity field
Superscript	
f	front
l	interface element

Subscripts	
i,j	matrix indexes
x,y	cartesian Directions
δ	delta Function
ρ	density
μ	viscosity
Ω	whole Domain
Γ	interface
α	number of Flow Dimensions
φ	scalar variable

1. INTRODUCTION

Multiphase flow problems include flows of solid particles in liquids or in gases, liquid droplets in gases, gas bubbles in liquids, and any combination of these. Applications of such flows are found in marine hydrodynamics, chemical, mineral, industrial, natural, and pollution control processes, etc. Some examples of such flows include: spray painting, spray combustion, boiling slurps, coal slurry transport, emulsion, cavitation, pneumatic conveying, sedimentation, atomization, fluidized bed, rain, snow, and volcanic rock motion. Although there has been a great deal of research conducted in this area of fluid mechanics, the complete dynamics of such flows is not fully understood due to their complex interphase coupling, whereby different phases may strongly affect one another (Taeibi-Rahni, 1995).

On the other hand, shock-bubble interaction is a multiphase flow problem. Computational simulation of this problem faces two challenges. First, discontinuity caused by the shock tube and second, discontinuity caused by different densities in the two phases of fluid. As follows, a preview of the efforts made to overcome each of these challenges is presented.

To deal with multiphase flows, various numerical schemes have been introduced and successfully implemented. To solve the full Navier-Stokes equations the marker and cell (MAC) method was developed via simulation of dam breaking problem (Harlow and Welch, 1995). In this method, distributed marker particles identify each fluid domain and the governing equations are solved using a projection method on a staggered grid. However, marker particles could make inaccuracies at fluid interfaces. So, in a newer method called volume of fluid (VOF), marker particles are replaced by marker functions, which indicate the location of the phases (Hirt and Nichols, 1981; Youngs, 1982; Ashgriz and Poo, 1991; Tryggvason *et al.*, 2011). The major problem with the original VOF method was crude reconstruction of the interface. Another method, which utilizes a continuous marker function, instead of the discontinuous one in VOF is level-set method, which was first presented by Osher and Sethian (1988). Level-set methods are robust and accurate in simulation of an interface evolution (Balabel 2012). In level-set method, the interface is identified by zero level of the level-set function.

Various newer methods arose from the concept of MAC and VOF methods. For instance, front-tracking method was introduced by Unverdi and Tryggvason (1992; 1992) for multi-fluid flows. They developed a successful method for viscous incompressible multiphase flows, using the Peskin's immersed boundary method (Peskin, 1977). Instead of reconstruction of interface location with the fluxes in and out of a partially filled cell to advect a marker function, the interface can be marked with advecting connected marker points and then the marker function can be reconstructed from the front location. The material properties, like viscosity and density, are advected by the markers and surface tension is computed. Other properties are computed in a fixed grid similar to VOF method. Richtmyer and Morton (1994) discussed the basic idea of front-tracking, but Glimm *et al.* (1988) developed algorithms based on front-tracking method. They represented the moving interface by a connected set of points to form a moving internal boundary.

In front-tracking method, topology changes in fluid interfaces, such as drops or bubbles coalescence or break up are not applied automatically, as in VOF method. Changes in the front points connection can be handled with higher code complexity. Besides, in the thin film between two interfaces, where it is in the order of the mesh size, interfaces may or may not properly approach together and thus, an additional control level may be needed (Tryggvason *et al.*, 2011).

The basic concept of front-tracking method, which is utilization of one set of conservation equations for the whole flow field, returns to the arrival time of CFD to Los Alamos (Tryggvason *et al.*, 1998). In this method, a fixed grid is used for the conservation equations and another lower dimension moving grid is applied to follow the interface between the fluids. The moving grid is generally denominated by the front (Tryggvason *et al.*, 2001). Since the interface is represented in Lagrangian fashion and the surface tension is implemented directly at the interface, the interface dynamics is captured explicitly in front-tracking method, while VOF and level set methods solve an advection equation to capture the interface in an Eulerian grid (Xie *et al.*, 2015). Front-tracking method is an explicit representation of the interface, therefore, the physical processes, such as deposition, diffusion, and chemical reactions can be naturally simulated using this method (Li *et al.*, 2010).

Front-tracking method has been used to simulate two and three-dimensional phase transition phenomena, such as precipitation, dissolution, freezing, and melting problems, with complex and changing interface geometry and topology. In such applications, the interface was propagated by the Lagrangian front-tracking method under the conservation laws of mass or energy coupled with an incompressible Navier-Stokes (Hu *et al.*, 2015). Siguenza *et al.* (2015) investigated a front-tracking immersed boundary method to solve the fluid-structure interactions between a capsule membrane and inner and outer fluids. Vu *et al.* (2015a, b) presented a front-tracking/finite difference method to simulate drop solidification on a cold plate and investigated the effects of affecting parameters on the solidification growth rate. The problem included solid–liquid, solid–air, and liquid–air interfaces that were explicitly tracked under the axisymmetric assumption. In addition, a two-dimensional non-linear, pressurization-rate dependent combustion ballistics was studied using front-tracking method (Hwang *et al.*, 2014).

Pivello *et al.* (2014) simulated an initially zigzagging bubble and an ascending bubble. They presented a fully adaptive front-tracking method for simulation of three-dimensional bubbly flows. An adaptive mesh refinement strategy was used to solve the Navier–Stokes equations with local detailing of the flow. The remeshing algorithm applied to the Lagrangian interface intrinsically preserved the geometry shape, dimensions, and the volume. The non-conservative interpolation of the velocity field entailed an additional algorithm for volume recovery.

De Jesus *et al.* (2015) presented a front-tracking/immersed boundary method (Ceniceros *et al.*, 2010a) with Eulerian adaptive mesh refinement abilities (Pivello *et al.*, 2014; Ceniceros *et al.*, 2010b) combined with a finite volume scheme (Lenz *et al.*, 2011) and a linear equation of state to simulate three-dimensional transient, incompressible two-phase flows with an insoluble surfactant.

Since density varies in compressible flows for each fluid, the governing equations must be solved to update the density field. Ghost fluid method (GFM), which captures fluid interfaces incompressible flows, has been developed using level-set technique to manage interfaces in an efficient and robust way. This is based on recognition of continuous and discontinuous variables, leading to a finite differencing across an interface. In this way, unphysical oscillations are avoided and smearing of discontinuous variables, such as entropy, is minimized (Fedkiw, 2001). Note, GFM is not a level-set method and it can easily be expanded to VOF or front-tracking formulations. The main properties of GFM are: simple implementation, easy extension to higher dimensions, and retention of sharp boundaries without smearing (Khazaeli *et al.*, 2013). GFM was used to implement sharp interface method for complex three-dimensional bodies (Mittal *et al.*, 2008). Pan (2010) developed GFM for simulation of heat transfer in incompressible flow over complex geometries. The complex shock-obstacle interaction was simulated using GFM (Chaudhuri *et al.*, 2011). GFM has been extended to the Navier-Stokes equations as well as to the Euler equations (Fedkiw *et al.*, 1998). Fedkiw *et al.* (1999) developed GFM for treating interfaces in Eulerian schemes. This method can be implemented effectively in finite difference discretization, since it includes jump condition. Liu *et al.* (2005) applied GFM to capture discontinuities in a compressible gas-water flow. GFM was used to capture strong shock impacting on a material interface (Liu *et al.*, 2003). It was also implemented in an elliptic interface problem (Liu *et al.*, 2000).

Several hybrid methods combine the best aspects of different ideas discussed above in a variety of ways in order to take the advantages of each method and to provide better solutions. To improve mass conservation problem in level-set method, Fedkiw *et al.* (1999) developed a ghost-fluid method, in which dummy values were assigned to grid points on the other side of the phase discontinuity. Shin and Juric (2002) proposed a hybrid front-tracking/level-set method for simulation of three-dimensional boiling flows. Aulisa *et al.* (2003) introduced a hybrid VOF/front-tracking method for interface advection and reconstruction in a two-dimensional space. A hybrid level-set/front-tracking algorithm was developed, using an unstructured mesh for two-phase flows involving complex domain geometries (Maric *et al.*, 2015).

In a shock tube rapidly, a shock wave travels into the low pressure region and a rarefaction or expansion wave travels into the high pressure region. A contact surface separates the quasi-steady flow areas behind these waves so that the velocity and pressure are the same. Various schemes have been developed to solve the Euler equations of gas dynamics for capturing the shock. However, the Godunov method and the original Roe schemes have been widely employed methods with high precision to simulate complex shock; they may fail or produce physically unrealistic numerical solutions for some problems (Perry and Imlay 1988; Roe 1981). Phongthanapanich (2009; 2013) proposed a mixed entropy and shock fixes method to improve numerical stability of the Roe flux-difference splitting scheme (RoeVLPA) on a two dimensional shock tube. The method combined the entropy fix methods of Van Leer *et al.* (1989) and Pandolfi and D'Ambrosio (2001) by modifying the original eigen values.

The main objective of this paper is to study two-dimensional shock-bubble interaction problems, using front-tracking/ghost-fluid method. One numerical method is infinite volume method with simple high resolution upwind scheme (SHUS). The results are presented for bubble with two different densities (helium and R22).

2. Computational Procedure

In this paper, we use front-tracking method, coupled with ghost-fluid method, to simulate the motion of fluid interfaces in some shock-bubble interaction problems. Shima and Jounouchi (1997) algorithm, simple high resolution upwind scheme (SHUS), was used for finding the numerical fluxes and higher-order spatial accuracy has been obtained, using MUSCL (Van Leer 1977; 1979). Also, time integration was performed using a third order TVD Runge-Kutta scheme (Gottlieb and Shu,1998).

2.1. Front Tracking Method

Unverdi and Tryggvason (1992) proposed a front-tracking method according to "one fluid model" and Peskin's immersed boundary method (Peskin 1977; 2002). In this method, the governing equations are to be solved in an Eulerian grid and the interface is tracked in a Lagrangian mesh. The velocity field is interpolated onto the Lagrangian mesh by delta function, δ. The force field is calculated on a Lagrangian mesh and is transferred to the fixed grid points. Grid communication was performed based on the immersed boundary method (Pivello *et al.*, 2014).

The conservative form of the Navier-Stokes equations used are:

$$\frac{\partial}{\partial t}(\rho\mathbf{u}) + \nabla\cdot(\rho\mathbf{uu}) = -\nabla p + \rho\mathbf{g} + \nabla(2\mu\mathbf{D}) + \sigma\kappa\mathbf{n}\delta(\mathbf{x}-\mathbf{x}^f), \tag{1}$$

where, ρ and μ are density and viscosity, **u** is velocity field, σ is surface tension coefficient, **n** is a unit normal to the interface, κ is interface curvature, and **g** is gravity acceleration. The delta function, δ, and the components of the deformation tensor rate **D** are defined as:

$$\delta(\mathbf{x}-\mathbf{x}^f) = \begin{cases} 0 & \mathbf{x} \neq \mathbf{x}^f \\ 1 & \mathbf{x} = \mathbf{x}^f \end{cases}, \tag{1}$$

$$D_{ij} = \frac{1}{2}\left(u_{i,j} + u_{j,i}\right). \tag{2}$$

Note, superscript *f* represents the front (the interface).

To avoid excessive numerical diffusion or oscillations around the interface due to the discontinuity of ρ and μ across the interface, an indicator function I(x,t) is introduced as an integral over the whole domain Ω(t) with the interface Γ(t) as:

$$I(\mathbf{x},t) = \int_{\Omega(t)} \delta(\mathbf{x}-\mathbf{x}')d\mathbf{v}'. \tag{3}$$

The above volume integral can as well be replaced by an integral over the interface:

$$\nabla I = \int_{\Gamma(t)} \mathbf{n}\delta(\mathbf{x}-\mathbf{x}')d\mathbf{s}. \tag{4}$$

To find the indicator function, a Poisson equation is required, as:

$$\nabla^2 I = \nabla\cdot\int_{\Gamma(t)} \mathbf{n}\delta(\mathbf{x}-\mathbf{x}')d\mathbf{s}. \tag{5}$$

Solving the above equation leads to the reconstruction of the indicator function. After determining this function, fluid properties, such as ρ and μ, can be found. To approximate the delta function, the distribution function can be applied, then the fraction of interface, such as σ, can be determined. The discretized form of the gradient function is introduced as (Unverdi and Tryggvason 1992):

$$\nabla I = \sum_{l} D\left(\mathbf{x} - \mathbf{x}^{(l)}\right)\mathbf{n}^{(l)}\Delta s^{(l)}, \tag{6}$$

where, superscript l denotes the interface element and distribution function D is proposed by Peskin (1977) as:

$$D\left(\mathbf{x} - \mathbf{x}^{(l)}\right) = \begin{cases} (4h)^{-\alpha}\prod_{i=1}^{\alpha}\left(1 + \cos\frac{\pi}{2h}\left(x_i - x_i^{(l)}\right)\right) & if \left|\mathbf{x}_i - \mathbf{x}_i^{(l)}\right| < 2h \\ 0 & otherwise, \end{cases} \tag{7}$$

where, h represents Eulerian mesh size and α is the number of flow dimensions.

Surface tension can be calculated after the material boundary advection. The Navier–Stokes equations can be integrated in time by any standard algorithm on the fixed grid (Fig. 1). The fixed grid is used for the conservation equations, while the moving grid of lower dimension marks the interface (Tryggvason *et al.*, 2001).

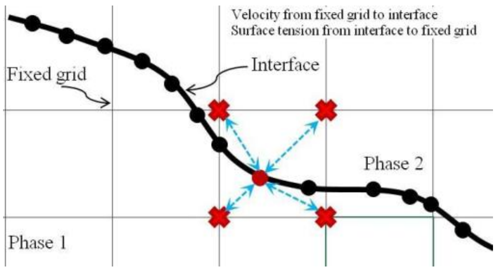

Fig. 1. Front-tracking method.

2.2. Ghost Fluid Method

Densities in each fluid in incompressible multiphase flow simulations are assumed to be fixed and can be updated using the front position. In this way, the accurate density jump at fluid interfaces is warranted. As stated before, in compressible flows, the density varies in each fluid and it must be updated using the solution of the governing equations.

Fedkiw *et al.* (1999) in their ghost fluid method define each fluid domain with its corresponding ghost fluid region and then the governing equations are solved in each fluid domain independently. At last, the solutions from both domains are merged together. In this way, the interface conditions are captured appropriately by defining a fluid that has velocity and pressure of the real fluid at each point of the flow, but entropy or density of the other fluid. These techniques provide capturing fluid interfaces in compressible flows, avoiding unphysical oscillations and minimizing the smearing of discontinuous variables.

Discontinuous variables across a fluid interface are given, using one-sided extrapolation; while variables such as velocity and pressure are copied from the real fluid (Fedkiw *et al.*, 1999). For extrapolation of discontinuous variables in ghost-fluid regions, the following advection equation has been used:

$$\frac{\partial \varphi}{\partial \tau} + n_x\frac{\partial \varphi}{\partial x} + n_y\frac{\partial \varphi}{\partial y} = 0, \tag{8}$$

where, φ is a scalar variable, such as entropy or a velocity component, while n_x and n_y are the components of a unit surface normal vector (Fedkiw *et al.*, 1999).

3. Physical Models

In this paper, the shock-bubble interaction problem was studied, using the front-tracking/ghost-fluid method in two dimensions, wherein two air-bubble shock-bubble interaction cases were considered. In both cases, a shock wave hits a bubble and then the bubble behavior is studied. In the first case, the bubble consists of helium which is lighter than air and was used for validating the numerical scheme. In the second case, the bubble consists of Refrigerant-22 (R22) which is heavier than air. Both cases are compared with the previous numerical and experimental studies.

3.1. Air-Helium Model

In order to study two-dimensional shock-bubble interaction, using front-tracking/ghost-fluid method, an air-helium shock-bubble interaction problem, investigated by many authors (Daramizadeh and Ansari, 2013; Terashima and Tryggvason, 2009; Haas and Sturtevant, 1987; Quirk and Karni, 1996; Bagabir and Drikakis, 2001; Razmi *et al.*, 2016a: 2017a, b, c; jafari *et al.*, 2017) was studied.

Figure 2 shows the computational domain, which consists of a two-dimensional cylindrical helium bubble in air. A shock wave with a Mach number of 1.22, initially at the right of the helium bubble, propagates from right to left and then hits the bubble. In addition, Table 1 shows the given geometrical parameters.

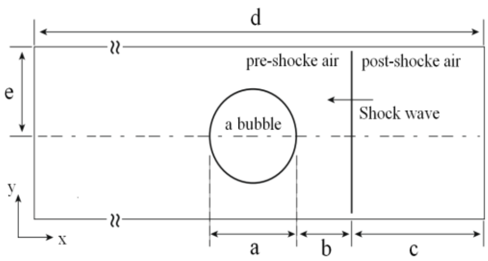

Fig. 2. Computational set-up.

Table 1 Given geometrical parameters

Parameter	a	b	c	d	e
Value [mm]	50	25	100	325	44. 5

Hence, the Euler equations were used as the governing equations and surface tension was ignored. In addition, zero gradient boundary condition was applied to the left and right boundaries, while slip-wall condition was used at the top and bottom boundaries. The Mach number of the incident shock wave was set to 1.22 and the non-dimensional initial conditions were as follows:

$$
\begin{aligned}
&\bar{\rho} = 1, \bar{u} = 0, \bar{p} = \frac{1}{\gamma_{air}}, \gamma_{air} = 1.4, \\
&\qquad \text{for pre} - \text{shocked air}, \\
&\bar{\rho} = 1.3764, \bar{u} = -0.3336, \bar{v} = 0, \bar{p} \\
&\qquad = \frac{1.5698}{\gamma_{air}}, \\
&\qquad \text{for poshocked air}, \\
&\bar{\rho} = 0.1819, \bar{u} = 0, \bar{v} = 0, \bar{p} = \frac{1}{\gamma_{air}}, \gamma_{helium} \\
&\qquad = 1.648, \\
&\qquad \text{for helium.}
\end{aligned} \tag{9}
$$

Note, speed of sound and bubble diameter were used for non-dimensionalization purposes. Also, the CFL number was set to 0.2.

3.2. Air-R22 Model

In order to study the interaction of a shock with a R22 bubble Haas and Sturtevant 1987; Quirk and Karni S 1996; Razmi *et al.,* 2016b; 2017d), the same geometry, bubble diameter, and conditions of the last model (i.e. air-helium case) was selected except that in this case, specific heat ratio and density of R22 bubble were considered as 1.249 and 3.15385 kg/m3, respectively.

4. Grid Independency Study and Code Validation

In this section, grid independency study and code validation will be discussed.

4.1. Grid Independency Study

As far as the optimized grid, as shown from Fig. 3 and 4, as the grid is refined from 301×83 to 601×165 and then to 901×247, more details of the bubble deformation is demonstrated. Note, because of symmetry, only the above half of the bubble is shown in Fig. 4. However, Fig. 5 shows that even with the 301×83 grid a relatively sensitive quantity, such as the position of upstream, downstream and jet points on the front (moving and deforming bubble), is resolved relatively accurate. To get the final results, in order to save CPU and for still more accurate results, we used the 601×165 grid.

4.2. Code Validation

Our code was validated separately for air-helium and air-R22 shock-bubble interaction problems. Comparison with other computational results (Terashima and Tryggvason 2009; Quirk and Karni S 1996; Bagabir and Drikakis 2001) is shown in Fig. 6, which shows relatively good agreements. Figure 6 shows distance-time plots at upstream, downstream, and jet for helium bubble at M=1. 22. Figure 7 shows time versus position diagram for interaction of a shock wave with a R22 cylindrical bubble and also a comparison with the other previous studies (Haas and Sturtevant 1987; Quirk and Karni 1996) This figure also shows relatively good agreements.

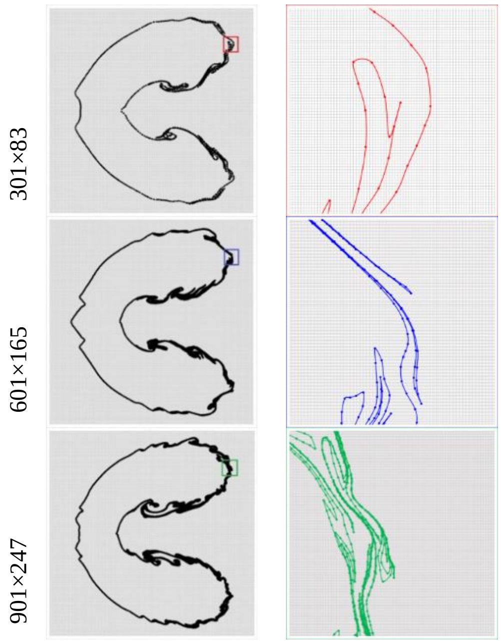

Fig. 3. Front shape for three different grids for air-helium shock-bubble interaction problem.

5. Results and Discussion

In this section, the results are presented and discussed for the two cases introduced before, namely air-helium and air-R22 models.

5.1. Air-Helium Shock-Bubble Interaction

Figure 8 shows a set of shadowgraphs comparing our study with the experimental results (Haas and Sturtevant 1987). When an incident Mach wave reaches a boundary, two main events occur: a portion of the wave reflects and returns towards the generating wave source and a portion transmit onward. According to Fig. 8, at 32 µsthe curved reflected wave on the right and the curved refracted wave inside the bubble connected to the incident shock wave are shown. Due to fact that speed of sound in helium is higher than that in air, the refracted wave travels faster than the incident wave and this is even more visible at 52 µs, where the two branches of the transmitted wave cross the incidentwave and the right side of the bubble has flattened because of the impact of the shock wave. At 62 µs, on the left side of the bubble, while the transmitted wave has joined the interface tangentially, a weak internal reflected wave emerges and a quadripartite shock junction is observed. At 72 µs, the transmitted wave moves completely outside the bubble and the internal reflected wave travels to the right. At 82 µs, the secondary transmitted wave diverges and its two branches cross each other. At 102 µs, the internal reflected wave backscatters to upstream and the incident shock wave diffracts

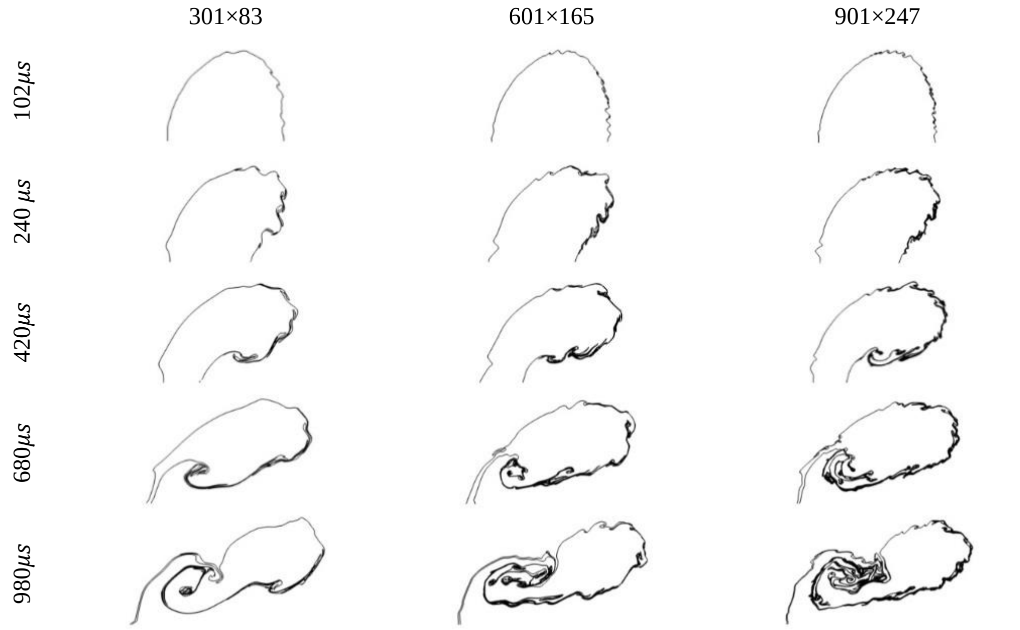

Fig. 4. Variation of the shape of the helium bubble with time for three different grids.

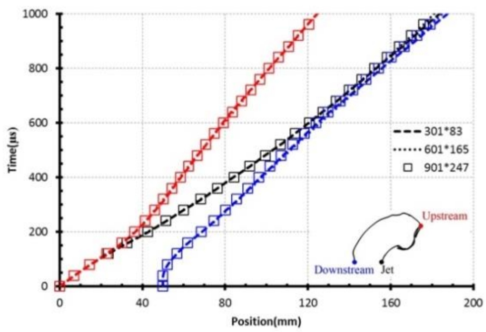

Fig. 5. Grid independency test.

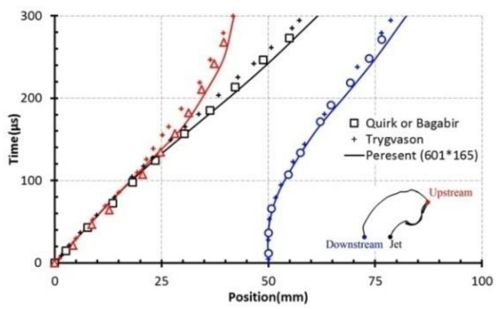

Fig. 6. Time versus position for air-helium shock-bubble interaction and comparison with other previous studies.

into downstream. Both the initial and secondary transmitted waves are merging. Meanwhile, the reflected waves from the walls are approaching the bubble from the top and bottom. The upstream interface of the helium bubble has almost flattened and the volume of the bubble has laterally grown. The deformation of the bubble continues so that by 245 μs, a beanshapedvolume can be observed. Thereafter, a jet of dense air forms leading to vertical structures at final steps of shock interaction (427 μs, 674 μs, and 983 μs). As it can be found, the total behavior of shock transmission, reflection, and the bubble deformation follow closely those of the experiment. Fif. 9 ti Fig. 11 shows the contours of density, Mach number and vorticity respectively. Two shock waves with two different strengths pass the cylindrical helium bubble. As it can be shown the stronger shock wave deforms the bubble in a shorter time. The bubble completely divides into two parts at about t=3.6s with interaction of a stonger shock wave M=1.5 while in the weaker shock case (M=1.22) at about t=7.3s. The different sensitivities to the changes have been shown in these three figures.

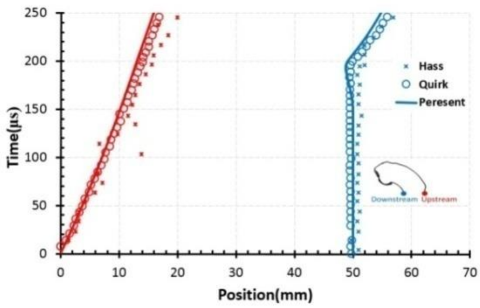

Fig. 7. Time versus position for air-R22 shock-bubble interaction and a comparison with other previous studies.

In this section, the numerical simulation results of interacting a shock with a bubble filled with R22 are discussed. R22 is a colorless gas which is

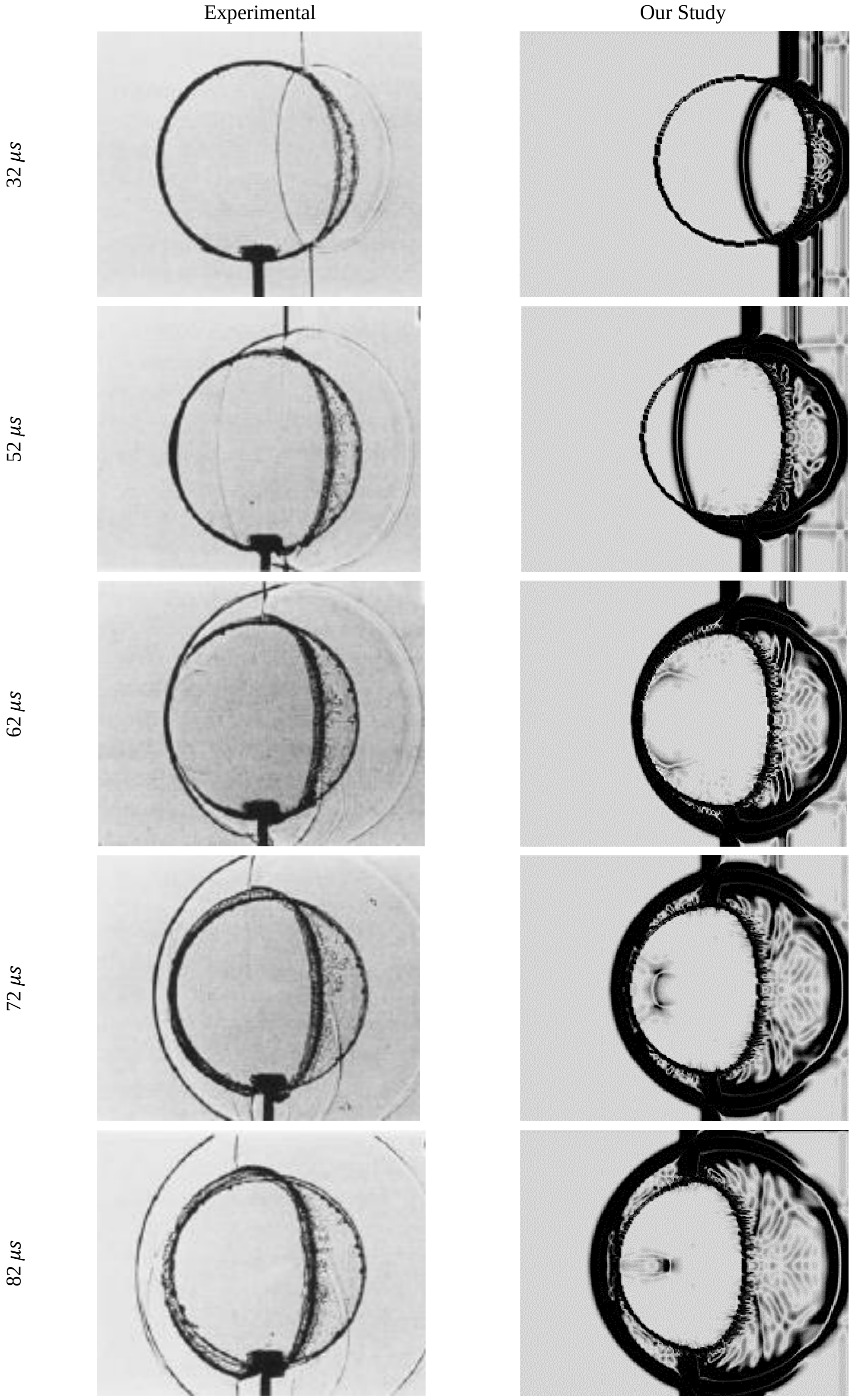

Fig. 8. Qualitative comparison between the experiment (Hass and Sturtevant 1987) and the present study. Interaction of a shock wave M=1.22 with a cylindrical helium bubble R=50 mm.

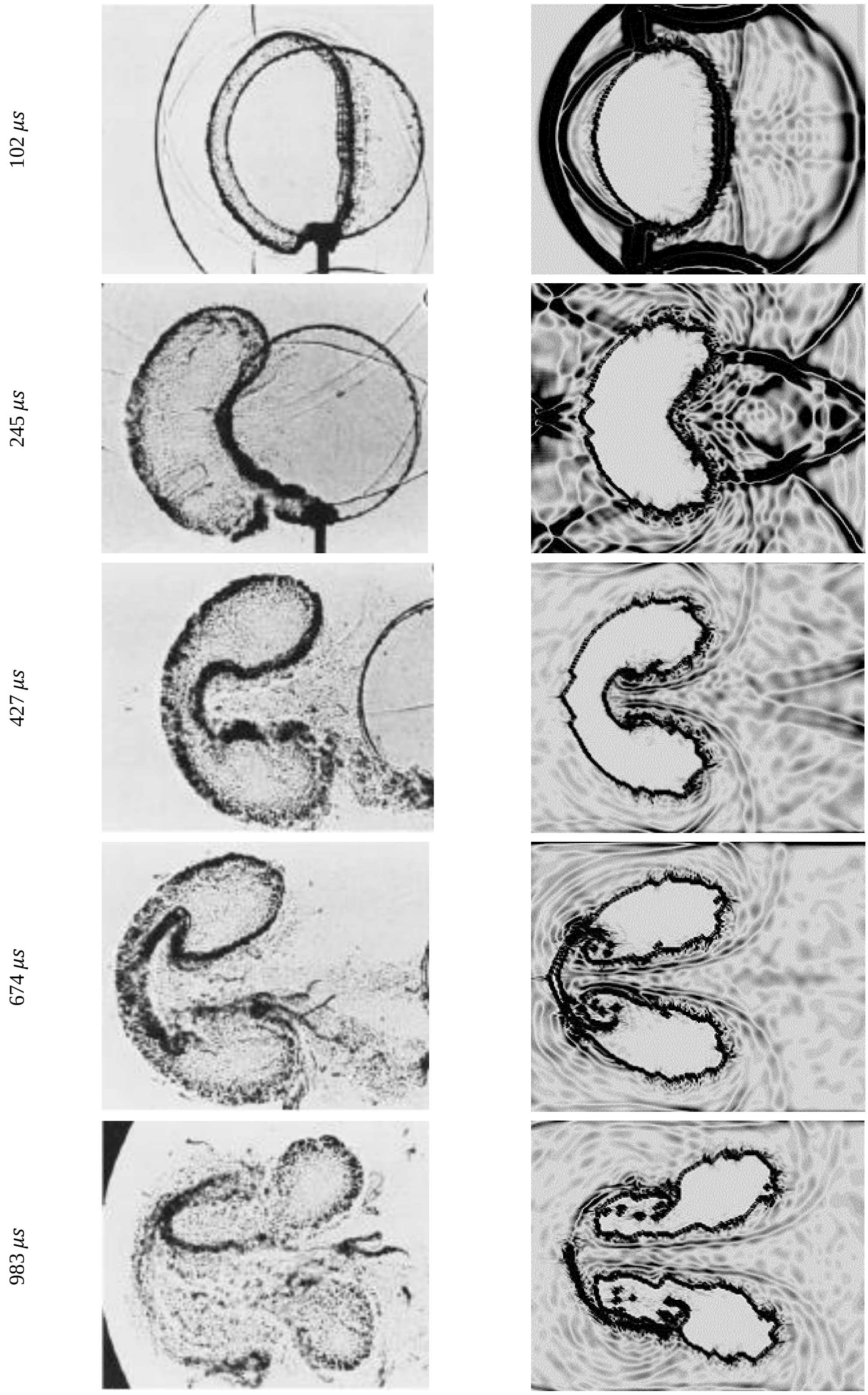

Fig. 8. Cont'd.

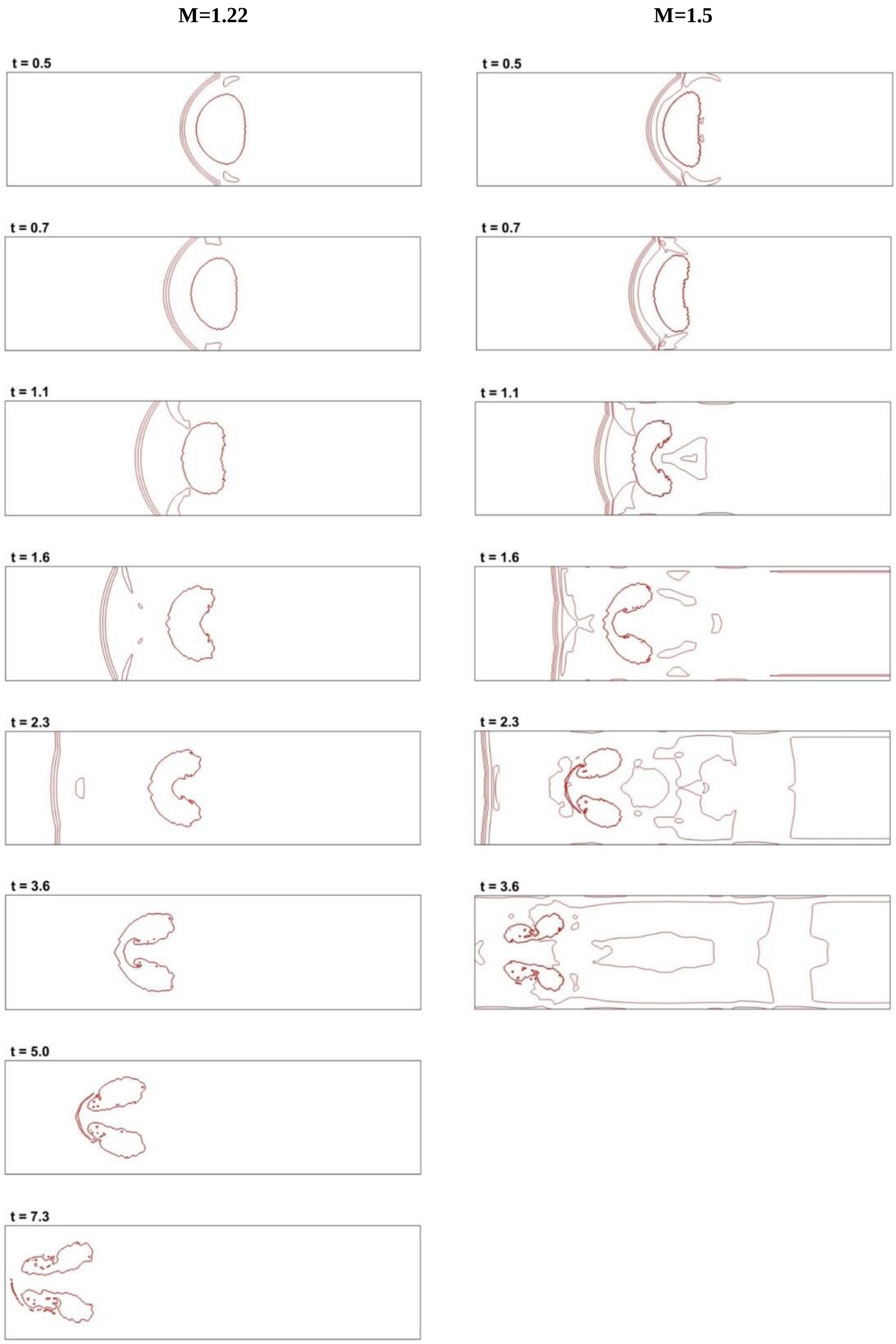

Fig. 9. Density contours after passing the shock waves with different Mach numbers (M=1.22 and 1.5) over a helium bubble.

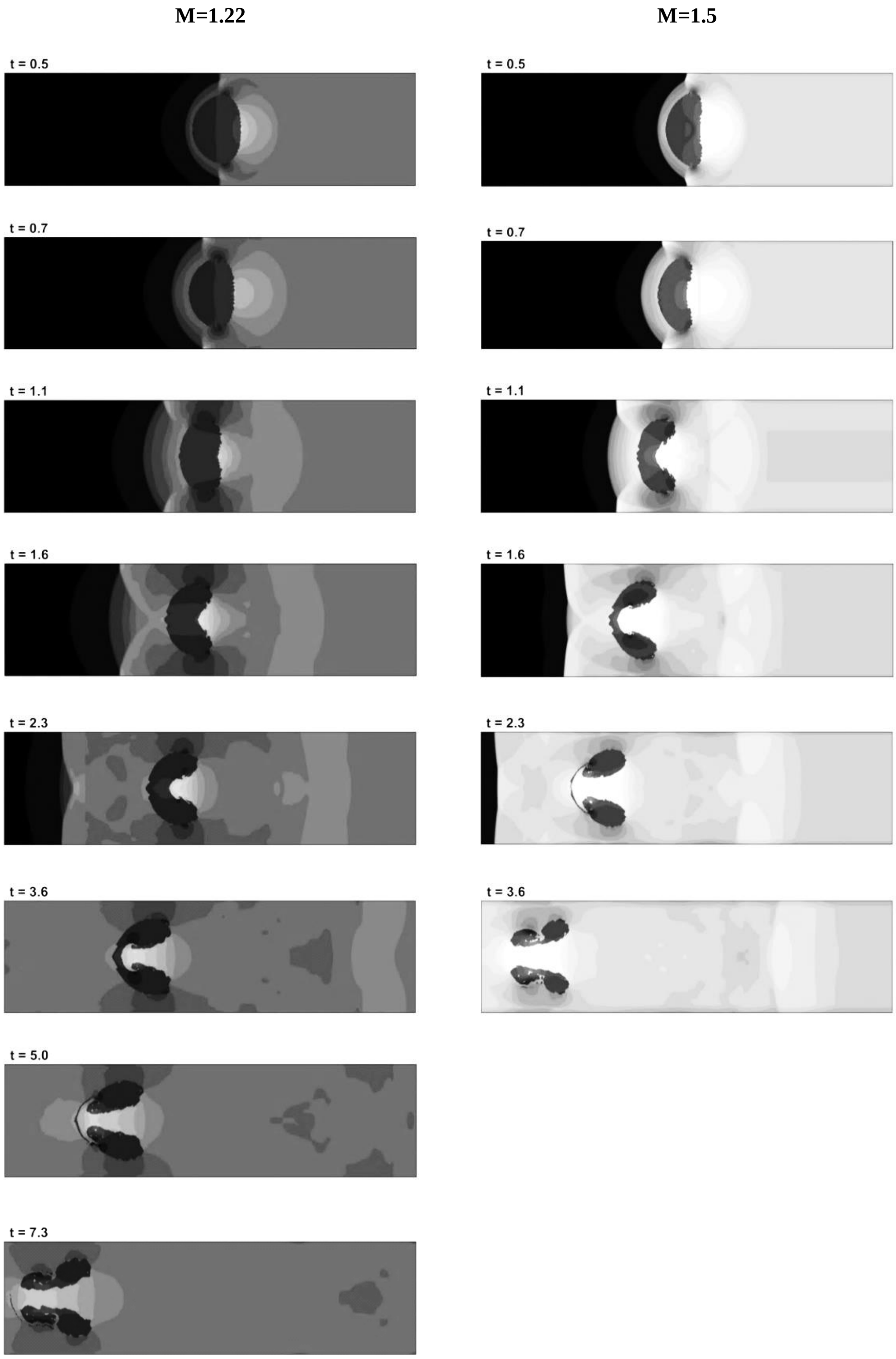

Fig. 10. Mach contours after passing the shock waves with different Mach numbers (M=1.22 and 1.5) over a helium bubble.

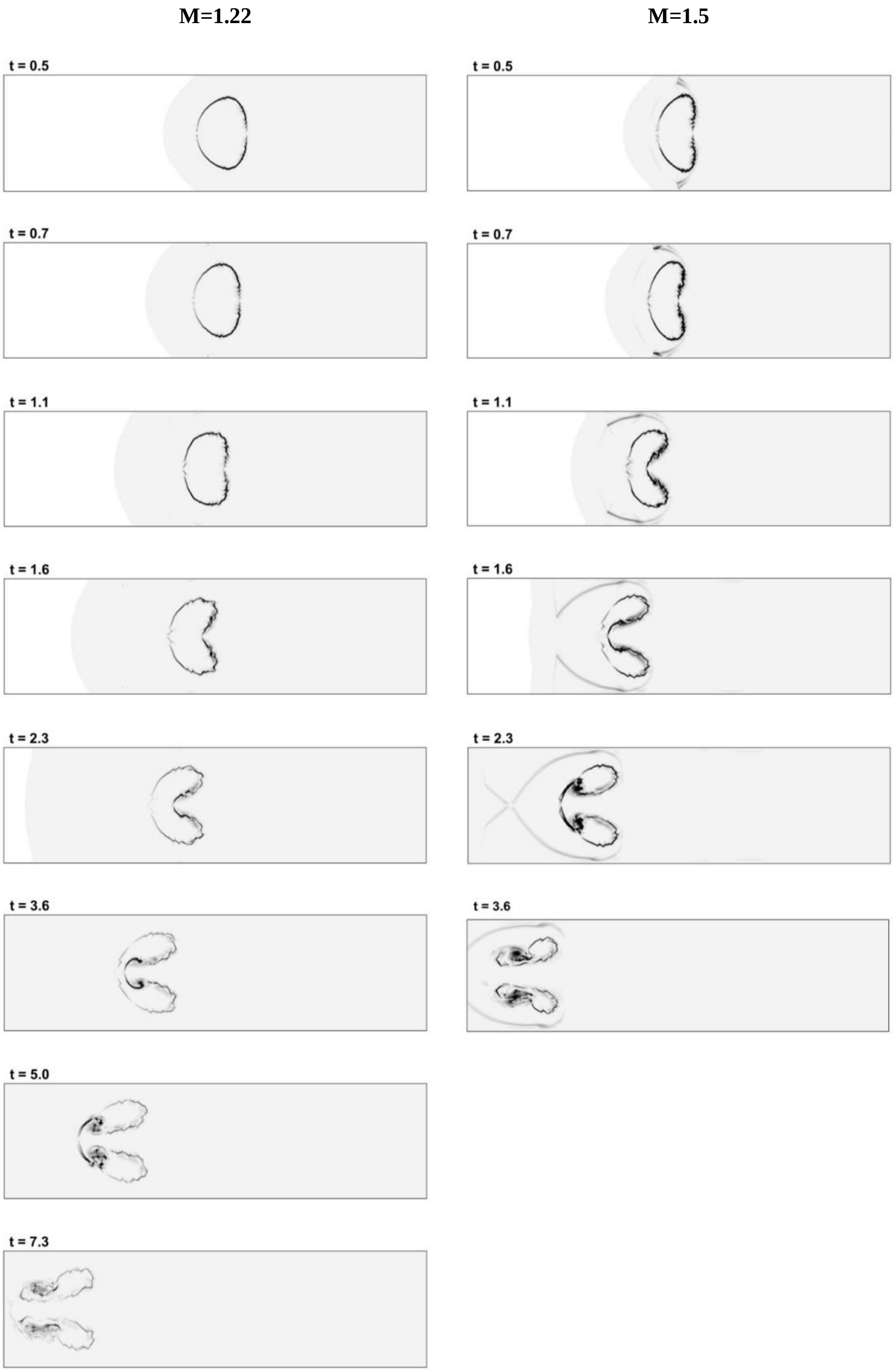

Fig. 11. Vorticty contours after passing the shock waves with different Mach numbers (M=1.22 and 1.5) over a helium bubble.

5.2. Air-R22 Shock Bubble Interaction

mostly used as propellant or refrigerant. It is a powerful greenhouse gas with a great global warming potential. Although, it is employed widely for air conditioning applications in developing countries, its use in developed countries has been restricted. R22 is heavier than helium and also air, so its dynamics while interacting with a shock would be different.

Figure 12 shows a series of shadowgraphs for this case (i. e. the interaction of a $\mathrm{M} = 1.22$shock wave

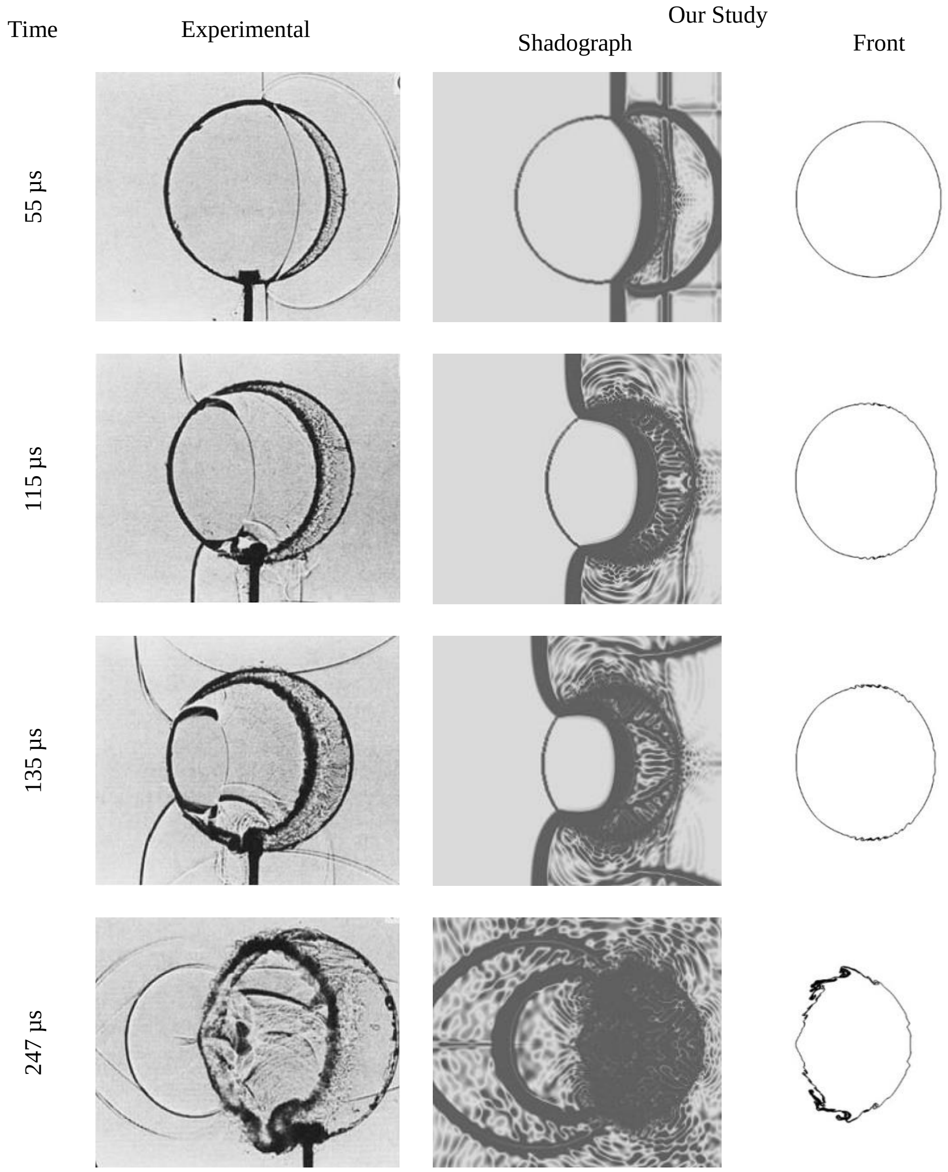

Fig. 12. Qualitative comparison between the experiment (Haas and Sturtevant 1987) and the present study. Interaction of a shock wave M=1. 22 with a cylindrical R22 bubble R=50mm.

witha R22 cylindrical bubble) compared with the experimental results of Haas and Sturtevant (1987). Referring to this figure, at 55 μs, the incident and the reflected shock waves are observed outside and the refracted wave inside the bubble travelling slower than the incident wave due to slower speed of sound in R22 medium. Also note that the bubble upstream interface has shifted from its initial position. At 115 μs, two internal diffracted wave fronts connect the incident shock to the refracted wave inside the bubble. At 135 μs, the reflected waves from the walls can be seen on the top and bottom of the bubble. By 247 μs, the two segments of the diffracted waves have crossed one another outside the bubble, and the refracted wave grows radially. A back-reflected wave can be observed inside the bubble at 342 μs and its back-transmitted wave at 417 μs. At 1020 μs, the bubble continues to grow laterally and changes into a pair of vortex.

6. Conclusion

To simulate fluid interface in shock-bubble interaction problem, an efficient front-tracking/ghost-fluid method was used. Defining interface conditions and using explicit front-tracking, using the ghost fluid method, the interface is captured relatively accurate. The test cases used were simulation of: a) an air-helium, and b) an air-R22 shock-bubble problem interactions.

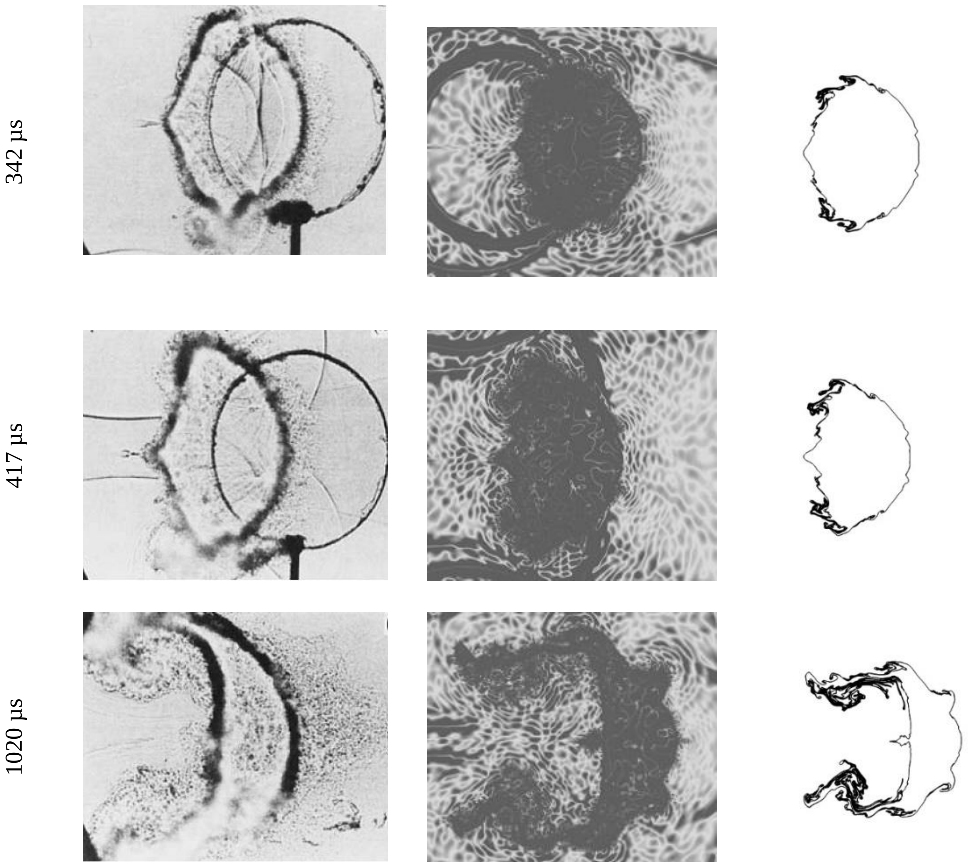

Fig. 12. Cont'd.

Our results were compared fairly well with other experimental reliable data. Thus, we demonstrated the high capability of the front-tracking/ghost-fluid method for simulation of complex fluid-fluid interfaces in complex compressible flows, especially in the presence of shock (e.g. shock-bubble interaction problem.

REFERENCES

Ashgriz, N. and J. Y. Poo (1991). FLAIR: Flux line-segment model for advection and interface reconstruction. *Journal of Computational Physics* 93, 449–468.

Aulisa, E., S. Manservisi, and R. Scardovelli (2003). A mixed markers and volume-of-fluid method for the reconstruction and advection of interfaces in two-phase and free-boundary flows. *Journal of Computational Physics* 188, 611-639.

Bagabir, A. and D. Drikakis (2001). Mach number effects on shock-bubble interaction, *Shock Waves* 11, 209-218.

Balabel, A. (2012). Numerical simulation of two-dimensional binary droplets collision outcomes using the level set method. *International Journal of Computational Fluid Dynamics* 26(1), 1-21.

Ceniceros, H. D., A .M. Roma, A. Silveira-Neto, and M. M. Villar (2010a). A. Robust, Fully Adaptive Hybrid Level-Set/Front-Tracking Method for Two-Phase Flows with an Accurate Surface Tension Computation. *Computational Physics* 8(1), 51-94.

Ceniceros, H. D., R. L. Nós, and A. M. Roma (2010b). Three-dimensional, fully adaptive simulations of phase-field fluid models. *Journal of Computational Physics* 229(17), 6135-6155.

Chaudhuri, A., A. Hadjadj, and A. Chinnayya (2011). On the use of immersed boundary methods for shock/obstacle interactions. *Journal of Computational Physics* 230(5), 1731–1748.

Daramizadeh, A. and M. Ansari (2013). Two-dimensional numerical simulation of shock-bubble interaction in compressible two-phase flows. *Amirkabir Journal Mechanical Engineering* 45(1), 1-13 (In Persian).

De Jesus, W. C., A. M. Roma, M. R. Pivello, M. M. Villar, and A. D. Silveira-Neto (2015). A 3d fronttracking approach for simulation of a two-phase fluid with insoluble surfactant. *Journal of Computational Physics* 281, 403 – 420.

Fedkiw, R. (2001) *Godunov Methods.* New York, Springer.

Fedkiw, R. and X. D. Liu (1998). The Ghost Fluid Method for viscous flows. In Hafez, M. (ed.), *Progress in Numerical Solutions of Partial Differential Equations*, Arachon, France.

Fedkiw, R., T. Aslam, B. Merriman, and S. Osher (1999). A non-oscillatory Eulerian approach to interfaces in multimaterial flows (the ghost fluid method). *Journal of Computational Physics* 152, 457–492.

Glimm, J., J. W. Grove, W. B. Lindquist, O. McBryan, and G. Tryggvason (1988). The bifurcation of tracked scalar waves. SIAM *J. Comput.* 9, 61–79.

Gottlieb, S. and C. W. Shu (1998). Total variation diminishing Runge-Kutta schemes. *Mathematics Computation* 67, 73-85.

Haas, J. and B. Sturtevant (1987). Interaction of weak shock waves with cylindrical and spherical gas in homogeneities. *Journal of Fluid Mechanics* 181, 41-76.

Harlow, F. H. and J. E. Welch (1965). Numerical Calculation of Time-Dependent Viscous Incompressible Flow of Fluid with Free Surface. *Physics of Fluids* 8, 21-82.

Hirt, C. W. and B. D. Nichols (1981). Volume of fluid (VOF) method for the dynamics of free boundaries. *Journal of Computational Physics* 39(1), 201-225.

Hu, Y., Q. Shi, V. F. De Almeida, and X. Li (2015). Numerical simulation of phase transition problems with explicit interface tracking. *Chemical Engineering Science* 128, 92-108.

Hwang, Y. H. and C. H. Chiang (2014). Tracking Methods to Study the Surface Regression of the Solid-Propellant Grain. *International Journal of Engineering and Technology Innovation* 4(4), 213-222.

Jafari, Y., A. Razmi, M. Taeibi-Rahni, and H. R. Massah (2017). Numerical Study of a Pulsating Bubble Behavior, Using a Hybrid Numerical Method, *The 3rd Congress of Acoustical Engineering Society of Iran*, Tehran, Iran (In Persian).

Khazaeli, R., S. Mortazavi, and M. Ashrafizaadeh (2013). Application of a ghost fluid approach for a thermal lattice Boltzmann method. *Journal of Computational Physics* 250, 126-140.

Lenz, M., S. F. Nemadjieu, and M. Rumpf (2011) A convergent finite volume scheme for diffusion on evolving surfaces. SIAM *Journal on Numerical Analysis* 49(1), 15-37.

Li, X., J. Glimm, X. Jiao, C. Peyser, and Y. Zhao (2010) Study of crystal growth and solute precipitation through front tracking method. *Acta Mathematica Scientia* 30(2), 377-390.

Liu, T. G., B. C. Khoo, and K. S. Yeo (2003). Ghost fluid method for strong shock impacting on material interface. *Journal of Computational Physics* 190, 651–681.

Liu, T. G., B. C. Khoo, C. W. Wang (2005). The ghost fluid method for compressible gas–water simulation. *Journal of Computational Physics* 204, 193–221.

Liu, X. D., R. Fedkiw, and M. Kang (2000). A boundary condition capturing method for Poisson equation on irregular domains. *Journal of Computational Physics* 160(1), 151-178.

Maric, T., H. Marschall, and D. Bother (2015). lentFoam – A hybrid Level Set/Front Tracking method on unstructured. *Computers & Fluids* 113, 20-31.

Mittal, R., H. Dong, M. Bozkurttas, F. M. Najjar, A. Vargas, and A. Von Loebbecke (2008). A versatile sharp interface immersed boundary method for incompressible flows with complex boundaries. *Journal of Computational Physics* 227(10), 4825-4852.

Osher, S. and J. A. Sethian, (1988). Fronts Propagating with Curvature Dependent Speed: Algorithms Based on Hamilton-Jacobi Formulations. *Journal of Computational Physics* 79, 12-49

Pan, D. (2010). A Simple and Accurate Ghost Cell Method for the Computation of Incompressible Flows Over Immersed Bodies with Heat Transfer. *Numerical Heat Transfer B* 58(1), 17-39.

Pandolfi, M. and D. D'Ambrosio (2001). Numerical Instabilities in Upwind Methods: Analysis and Cures for the “Carbuncle” Phenomenon. *Journal of Computational Physics* 166(2), 271-301.

Perry, K. M. and S. T. Imlay (1988). Blunt-body flow simulations. *AIAA paper*, 88-2904.

Peskin, C. S. (1977). Numerical analysis of blood flow in the heart, *Journal of Computational Physics* 25(3), 220–252.

Peskin, C. S. (2002). The immersed boundary method. *Actanumerica* 11, 479-517.

Phongthanapanich, S. (2013). Study of Shock Tube Problem on Two-dimensional Triangular Grids by means of RoeVLPA Scheme. AIJSTPME 6(3), 75-81.

Phongthanapanich, S. and P. Dechaumphai (2009). Healing of shock instability for Roe’s flux-difference splitting scheme on triangular meshes. *International Journal Numerical Methods Fluids* 59(5), 559–575.

Pivello, M. R., M. M. Villar, R. Serfaty, A. M. Roma, and A. Silveira-Neto (2014). A fully adaptive front tracking method for the simulation of two phase flows, *International Journal of Multiphase Flow* 58, 72-82.

Quirk, J. and S. Karni (1996). On the dynamics of a shock–bubble interaction. *Journal of Fluid Mechanics* 318, 129-163.

Razmi, A., Y. Jafari, H. Ahmadian, A. R. Agha Ali

Mesgar, M. Taeibi-Rahni, and H. R. Massah (2017a). Computational Investigation of Mach Number Effects on Density Changes in a Helium-Air Shock Tube, Using a Front-Tracking/Ghost-Fluid Method, *The 3rd Congress of Acoustical Engineering Society of Iran*, Tehran, Iran.

Razmi, A., Y. Jafari, M. Taeibi-Rahni, and H. R. Massah (2017d). Numerical Study of a R22-Air Shock Tube, Using Front-Tracking/Ghost-Fluid Method", The 2nd International Conference on Mechanical and Aerospace Engineering, Tehran, Iran.

Razmi, A., Y. Jafari, M. Taeibi-Rahni, and H. R. Massah (2016a). Computational Investigation of Mach Number Effects on Helium-Air Shock Tube Problem, Using a Hybrid Front-Tracking/Ghost-Fluid Method, *The 2nd International Congress on Technology Engineering & Science*, July 28-29, Kuala Lumpur, Malaysia.

Razmi, A., Y. Jafari, M. Taeibi-Rahni, and H. R. Massah (2016b). Numerical Simulation of the Interaction of Weak Shock Waves with a Cylindrical R22 Bubble, Using a Hybrid Front-Tracking/Ghost-Fluid Method, *The 2nd International Congress on Technology Engineering & Science*, July 28-29, Kuala Lumpur, Malaysia.

Razmi, A., Y. Jafari, M. Taeibi-Rahni, and H. R. Massah (2017b). Numerical Simulation of a Helium-Air Shock Tube, Using a Hybrid Numerical Method, *The 2nd International Conference on Mechanical and Aerospace Engineering*, Tehran, Iran.

Razmi, A., Y. Jafari, M. Taeibi-Rahni, and H. R. Massah (2017c). Computational Investigation of the Shock Wave Strength Effect on Mach Contours in a Helium Bubble Passed a Shock Wave, *The 2nd International Conference on Mechanical and Aerospace Engineering, Tehran*, Iran (In Persian).

Richtmyer, R. D. and K. W. Morton (1994). *Difference methods for initial-value problems*. 2nd edition, Krieger Publishing Company Malabar.

Roe, P. L. (1981). Approximate Riemann Solvers, Parameter Vectors and Differencing Scheme. Journal of Computational Physics 43, 357-372.

Shima, E. and T. Jounouchi (1997). Role of CFD in Aeronautical Engineering (No.14) - AUSM Type Upwind Schemes. NAL SP-34, 7-12.

Shin, S. and D. Juric (2002). Modelling three-dimensional multiphase flow using a level contour reconstruction method for front tracking without connectivity. *Journal of Computational Physics* 180, 427–470.

Siguenza, J., R. Mozul, F. Dubois, D. Ambard, S. Mendez, and F. Nicoud (2015). *Numerical methods for modeling the mechanics of flowing capsules using a front-tracking immersed boundary method*, Procedia IUTAM 00.

Taeibi-Rahni, M. (1995). *Direct Numerical Simulation of Large Bubbles in a Free Shear Layer* (Ph.D Dissertation). Illinois, University of Illinois at Urbana-Champaign.

Terashima, H. and G. Tryggvason (2009). A front-tracking/ghost-fluid method for fluid interfaces in compressible flows. *Journal of Computational Physics* 228(11), 4012-4037.

Tryggvason, G., B. Bunner, A. Esmaeeli, D. Juric, N. Al-Rawahi, W. Tauber, and Y. J. Jan (2001). A Front-Tracking Method for the Computations of Multiphase Flow. *Journal of Computational Physics* 169(2), 708-759.

Tryggvason, G., B. Bunner, O. Ebrat, and W. Tauber (1998). Computations of multiphase flows by a finite difference/front tracking method. I. Multi-fluid flows. *In: 29th Computational Fluid Dynamics*, Lecture Series 1998-03, Von Karman Institute for Fluid Dynamics.

Tryggvason, G., R. Scardovelli, and S. Zaleski (2011) *Direct numerical simulations of gas–liquid multiphase flows. Cambridge*, Cambridge University Press.

Unverdi, S. O. and G. Tryggvason (1992). A front-tracking method for viscous, incompressible, multi-fluid flows. *Journal of Computational Physics* 100 (1), 25-37.

Van Leer, B. (1977). Towards the ultimate conservative difference scheme. IV. A new approach to numerical convection, *Journal of Computational Physics* 23, 276–299.

Van Leer, B. (1979). Towards the ultimate conservative difference scheme. V. A second-order sequel to Godunov's metho. *Journal of Computational Physics* 32, 101–136.

Van Leer, B., W. T. Lee, and K. G. Powell (1989). Sonic-Point Capturing. *AIAA 9th Computational Fluid Dynamics Conference*, AIAA Paper-89- 1945-CP, Buffalo, New York.

Vu, T. V., G. Tryggvason, S. Homma, and J. C. Wells (2015a). Numerical investigations of drop solidification on a cold plate in the presence of volume change. *International Journal of Multiphase Flow* 76, 73-85.

Vu, T. V., G. Tryggvason, S. Homma, J. C. Wells, and H. Takakura (2015b). Front Tracking Computation of Trijunction Solidification with Volume Change. *Procedia IUTAM* 15, 14-17.

Xie, H. Q., Z. Zeng, and L. Q. Zhang (2015). Three-dimensional multi-relaxation-time lattice Boltzmann front-tracking method for two-phase flow. *Chinese Physics* B 25, 014702.

Youngs, D. L. (1982). Time-Dependent Multi-Material Flow with Large Fluid Distortion. *Numerical Methods for Fluid Dynamics* 24(2), 273–285.